Large-Scale 3D Random Finite Element Analysis of Embankment Seepage Stability

Yong Liu[1(✉)], Man-Yu Wang[1], Yu-Tao Pan[2], and Kai Yao[3]

[1] State Key Laboratory of Water Resources and Hydropower Engineering Science, Institute of Engineering Risk and Disaster Prevention, Wuhan University, 299 Bayi Road, Wuhan 430072, People's Republic of China
`liuy203@whu.edu.cn`
[2] Department of Civil and Environmental Engineering, Norwegian University of Science and Technology, Høgskoleringen 7a, 7491 Trondheim, Norway
[3] School of Qilu Transportation, Shandong University, 12550 East Second Ring Road, Jinan 250002, People's Republic of China

Abstract. The stability assessment of a soil embankment in the flooding season has attracted increasing attention in recent years. The current study performs a coupled hydraulic-mechanical analysis of an embankment subjected to water level fluctuation. The coefficient of permeability of embankment soils is represented by a uniform random field with upper and lower bounds. The random finite element method is incorporated for the solution of such coupled analysis. The results indicate that the horizontal correlation length of the permeability field has significant effects on the seepage patterns, leading to a greater variability in the total flow rate, since water flows more easily along the regions of higher permeability. In addition, the failure mechanism resulted from the coupled analysis shows that a rise of water level plays a predominant role in the instability of the embankment, compared with the generated irregular seepage force. The factor of safety of the embankment decreases with the increase of upstream water level, and the corresponding failure mode also changes significantly. The findings from this study can serve as a guidance for the design or reinforcement of a soil embankment and provide a new insight into the solution of green life cycle and sustainable development of embankment engineering.

Keywords: Soil embankment · Heterogeneous permeability · Flow rate · Coupled hydraulic-mechanical analysis · Random finite element method

1 Introduction

A long soil embankment plays a vital role in preventing the water flow for flood protection purposes. However, the rise of water level caused by the continuing rainstorm may pose a great threat to the overall stability of an embankment composed of untreated natural soils (Jia et al. 2009; Gholami Korzani et al. 2018; Li et al. 2018). Once a failure of embankment occurs, the environment will be affected to a greater extent and the caused loss is unpredictable, such as the occurred events as shown in Fig. 1. In recent

years, increasing relevant events of collapse of a long embankment resulting from the seepage failure were widely reported (Rivera-Hernandez et al. 2019). For instance, such typical events of embankment breaching have taken place in the Poyang Lake regions of China in July 2020 (see Fig. 2), which caused irreparable losses to the agriculture and increased hidden dangers in terms of the stability of buildings. The process of such a failure is essentially a typical coupled hydraulic-mechanical problem defined in numerical investigation (Qi and Vanapalli 2015; Zhang et al. 2018). Many studies associated with this issue were carried out to tentatively seek an acceptable solution so that making it possible to clearly describe the coupled mechanism involved (Cho 2012; Rivera-Hernandez et al. 2019).

In general, the spatial distribution of porosity in natural soil mass is extremely uneven due mainly to the complexity of geo-structures, which may lead to a larger uncertainty in the hydraulic properties of soils compared with other mechanical parameters (Srivastava et al. 2010). In literature, it is found that the coefficient of permeability of most types of soils often covers two or more orders of magnitude (Swiss Standard SN 670 010b 1999), which means that it encounters a difficult in accounting for the spatial variability of soil permeability in a reliable way. Cho (2012) has examined the effects of uncertainty due to the spatial heterogeneity of soil permeability on the seepage flow through the dam and soil foundation, where the saturated hydraulic conductivity of soils was represented by a two-dimensional (2D) lognormal random field. However, the variation range of the random values generated from a marginal lognormal distribution is grossly limited; thus, it expects that a clear range of its values should be reflected (Fenton and Griffiths 2008). Moreover, the analysis of an embankment is essentially a three-dimensional (3D) numerical problem that cannot be neglected in the examination of failure mechanism; however, investigation related to this 3D issue is rarely covered in the previous studies (e.g. Griffiths and Fenton 1997). For such a large-scale analysis, the required efficiency also depends greatly on the representation method for the spatially variable soils. As such, these challenges form the motivation of the current study.

The intention of this work is to evaluate the performance of a large-scale 3D soil embankment subjected to water level fluctuation where the spatial heterogeneity of soil permeability is considered. The random finite element method is employed herein to obtain a relatively accurate solution of the output responses. Uncertainty of flow rate resulted from the spatially variable soil permeability is estimated by the probabilistic approach. The corresponding seepage pattern and failure mechanism under various combined conditions are also evaluated in detail.

Fig. 1. Failures of soil embankments from the field observation (a) Event 1 occurred in Xinjiang, China, February 2013 (Chen 2013) and (b) Event 2 occurred in Guangdong, China, May 2014 (Yu 2014).

Fig. 2. Typical events of embankment breaching due to continuous heavy rainfall taken place in the Poyang Lake regions of China in July 2020 (Chen 2020).

2   Governing Equations of Coupled Hydraulic-Mechanical Analysis

The coupled solutions related to the soil structure and water flow are required to simulate the process of seepage and deformation in a soil embankment (Zhang et al. 2018). The force equilibrium equations for a saturated soil in 3D condition can be expressed as:

$$
\begin{cases}
\dfrac{\partial \sigma_x}{\partial x} + \dfrac{\partial \tau_{xy}}{\partial y} + \dfrac{\partial \tau_{xz}}{\partial z} + b_x = 0 \\[2mm]
\dfrac{\partial \tau_{yx}}{\partial x} + \dfrac{\partial \sigma_y}{\partial y} + \dfrac{\partial \tau_{yz}}{\partial z} + b_y = 0 \\[2mm]
\dfrac{\partial \tau_{zx}}{\partial x} + \dfrac{\partial \tau_{zy}}{\partial y} + \dfrac{\partial \sigma_z}{\partial z} + b_z = 0
\end{cases}
\tag{1}
$$

where σ_x, σ_y, and σ_y are the total normal stresses in the x-, y-, and z-directions, respectively; τ_{xy} is the shear stress on the x-plane in the y-direction ($\tau_{xy} = \tau_{yx}$), and τ_{yz} and τ_{zx} are similar to the former; b_x, b_y, and b_z are the body forces in the x-, y-, and z-directions, respectively. For the saturated soils, the effective stress state variable is used in the coupled analysis:

$$
\sigma' = \sigma - u_a + \chi(u_a - u_w)
\tag{2}
$$

where σ' is the effective stress; u_a is the pore air pressure, which is equal to zero in this study; u_w is the pore water pressure, and $(u_a - u_w)$ is the matric suction; χ is assumed to be equal to degree of saturation (i.e. equal to 1.0). Based on the effective stress, the modified Mohr-Coulomb failure criterion for the shear strength of saturated soils can be written as:

$$
\tau_f = c' + (\sigma - u_w)\tan \varphi'
\tag{3}
$$

where τ_f is the shear strength; c' is the effective cohesion and φ' is the effective friction angle. Based on the balance of pore water and the Darcy's law, the governing equation

for steady water flow through saturated soils based on mass conservation can be written as:

$$\frac{\partial^2 H}{\partial x^2} + \frac{\partial^2 H}{\partial y^2} + \frac{\partial^2 H}{\partial z^2} = 0 \tag{4}$$

where H is the hydraulic head. Combined with the given boundary conditions, the above equations reflecting the coupled mechanism are solved numerically by using finite element method within a prescribed number of iterations.

3 Methodology

3.1 Modelling of Soil Embankment

This work extends the 2D embankment studied by Cho (2012) to a long idealized 3D model whose geometric profile and finite element mesh are shown in Fig. 3. The embankment with a height of 5 m and a length of 50 m is constructed on a 5 m thick soil foundation. Two stable upstream water levels of 7 m and 9 m are considered to reflect the fluctuation of water level during the rainstorm period. A fine mesh schedule with 250,460 eight-node brick pore pressure elements is discretized to meet the accuracy requirement of coupled analysis. The four sides of the model are on vertical rollers preventing movement in their vertical directions. the bottom of the mesh is fixed in all directions. Some distances away from the slope toe are placed to minimize the influence of displacement boundary on the failure mechanism. For the seepage boundary conditions, the upstream surfaces below the water level and the downstream flat surface are considered as permeable boundaries.

The soil property of the embankment is treated as the same as that of foundation layer due to the consideration of high similarity of soil materials in an adjacent site. The finite element model idealizes the soils as an elastic-perfectly plastic porous material with the Mohr-Coulomb failure criterion. The present research mainly focuses on the seepage behavior of a soil embankment where the permeability is modelled as spatially random; thus, for simplicity the effective shear strength parameters are assumed to be deterministic. The soil parameters used for the coupled analysis are listed in Table 1.
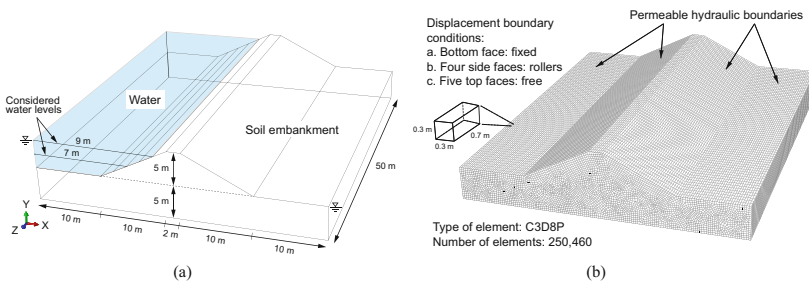

Fig. 3. (a) Profile of the embankment geometry; (b) displacement and seepage boundary conditions of the finite element model.

Table 1. Parameters of soil properties

Parameter	Unit	Symbol	Value
(a) Deterministic parameters			
Effective cohesion	kPa	c'	10
Effective friction angle	degree	φ'	15
Young's modulus	kPa	E	10^4
Poisson's ratio	—	v	0.3
Unit weight of water	kN/m^3	γ	10.0
(b) Statistical property of coefficient of permeability of soils			
Coefficient of permeability	m/s	k	$5.0 \times 10^{-6} - 5.0 \times 10^{-4}$
Arithmetic average of k	m/s	—	2.5×10^{-4}
Vertical correlation length of k	m	θ_v	2
Horizontal correlation length of k	m	θ_h	5, 10, 20

3.2 Spatial Variability of Soil Permeability

In this study, the spatial variability of the saturated coefficient of permeability of soils is represented by a 3D uniformly distributed random field, defined by its predefined upper and lower bounds and a correlation structure. The considered bounds for its value range from 5.0×10^{-6} to 5.0×10^{-4} m/s, and the corresponding correlation lengths are also listed in Table 1b. The random field with a marginal uniform distribution is generated through the translation approach (Grigoriu 1995), where the underlying Gaussian random field with a squared exponential auto-correlation structure is first generated by the modified linear estimation method (Liu et al. 2014). The reason for adopting a uniformly distributed random field in this study is that, for most types of soils its value of coefficient of permeability often covers several orders of magnitude (Swiss Standard SN 670 010b 1999), and the likelihood of each value involved in this range is considered to be equal in order to reduce the influence caused by its excessive variability. This is a major advantage relative to the use of a lognormal distribution in modelling the spatial heterogeneity of soil permeability, although the lognormal one has been widely used in previous similar studies (e.g. Cho 2012).

In geotechnical engineering, the vertical correlation length of soil properties often varies in a small domain relative to model geometry and may easily be estimated from in situ measured data, whereas the horizontal correlation length is generally much larger than the vertical one and more challenging to be quantified in a reliable way (Phoon and Kulhawy 1999). For this reason, the vertical correlation length of the permeability field remains constant, while the horizontal one varies in the parametric studies.

3.3   Description of Coupled Process

The numerical coupled process involved in this study consists of two main analysis steps. With the given seepage boundaries, a steady-state seepage analysis incorporated with the generated random field is first performed to gain the contours of pore water pressure and to calculate the total flow rate through the embankment. After determining the pore pressure at each integration point, the stress distribution can then be computed according to the principle of effective stress. At this stage, a static analysis step is set to evaluate the stability of the embankment within the predefined iteration numbers. The strength reduction technique widely used for the problems of slope stability is employed to obtain the minimum factor of safety of the embankment. Details of this technique can refer to the work by Wang et al. (2020). The non-convergence of the finite element program is herein taken as a basis for determining the occurrence of instability of an embankment.

3.4   Monte Carlo Simulation

A reliable estimation of the flow rate is necessary for the seepage behavior of a soil embankment when taking the spatial variability of permeability into account. The Monte Carlo simulation is performed due to its better robustness compared with other probabilistic methods (Fenton and Griffiths 2008). In a Monte Carlo simulation, the random permeability filed varies from one realization to the next, and this process should be repeated to obtain the statistical properties of the flow rate. The convergence result of the statistics of normalized flow rate shown in Fig. 4, based on the embankment models with a 7 m water level but under various correlation lengths, indicates that 100 times of simulation is sufficient to obtain an acceptable consequence. On the other hand, for the large-scale 3D finite element model analyzed in this study, the Monte Carlo technique requires a large amount of computational efforts, but it can be completed through the parallel computing on a high-performance workstation.
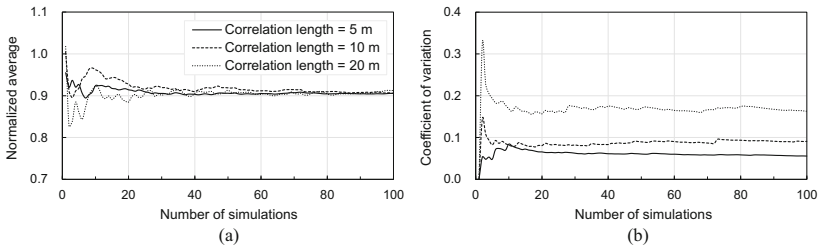

Fig. 4. Convergence check of Monte Carlo simulations by plotting the statistics of normalized flow rate (a) average and (b) coefficient of variation as a function of the number of simulations based on the cases with a 7 m upstream water level but under various correlation lengths.

4   Results and Discussion

4.1   Deterministic Analysis

Prior to probabilistic investigations, a deterministic coupled analysis is performed with a fixed coefficient of permeability of 2.5×10^{-4} m/s at the arithmetic average of the uniform distribution. Although the results of a 3D deterministic analysis may be basically identical to that from a 2D case, it can assess the ability of the numerical analysis to predict the coupled behaviors associated with the failure mechanism of a soil embankment.

Figure 5 shows the vectors of seepage velocity in the deterministic embankment soils under two sets of upstream water levels. For simplicity only half of the entire model is herein presented (i.e. 25 m in the axis direction). It can be seen that the water flow within embankment follows a common seepage pattern encountered in general cases. From the observations at the downstream exit, for each vertical cross section the seepage patterns are the same as each other, verifying the viewpoint that a 2D coupled analysis is considered reasonable and accurate enough if only the deterministic soil is analyzed. The computed total flow rate passing through the 3D embankment obtained with the finite element method, for upstream water levels with 7 m and 9 m, respectively, are 28.5 m^3/h and 68.2 m^3/h. Moreover, since the entire embankment soil is assumed to be at a saturated state under rainstorm conditions, a part of water flow above the phreatic line can be observed apparently. By comparing the two cases presented in Fig. 5, the rise of water level varying from 7 m to 9 m significantly raises the positon of the outflow, forming a free outflow surface at the downstream slope of the embankment as shown in Fig. 5b. These observations resulting from the 3D deterministic analyses give a reasonable approximation to the coupled performance of a large-scale embankment, which offers a solid basis for the random finite element analysis.
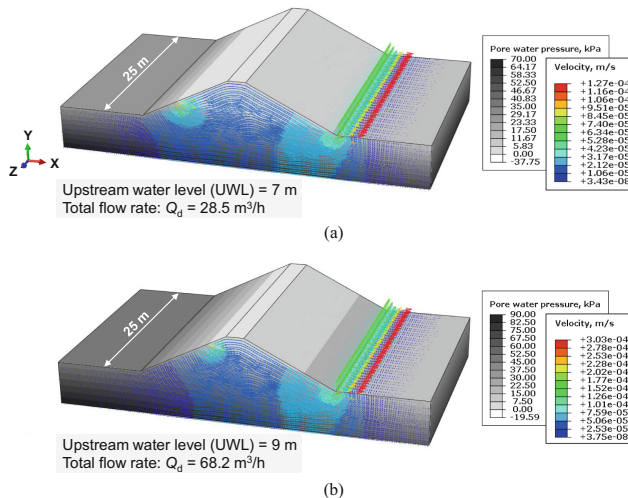

Fig. 5. Distribution of pore water pressure and vectors of seepage velocity in deterministic soils for the embankment with an upstream water level of (a) 7 m and (b) 9 m.

4.2   Estimation of Total Flow Rate Through Embankment

In this section, a parametric study on the horizontal correlation length of the 3D uniformly distributed random field is carried out to estimate the quantity of the flow rate through the embankment. Each realization of random field for the cases with the same correlation length but different water levels are identical to guarantee the consistency of the site.

Figure 6 shows the effects of horizontal correlation length θ_h on the histograms of normalized total flow rate for embankments under different water levels. Without loss of generality, for simplicity all the results of flow rate obtained from random models are normalized by the corresponding deterministic result marked as the vertical dotted line in those graphs. Only the results of these cases with a water level of 7 m are illustrated due to its similarity in histogram distributions with that of 9 m water level. For a small correlation length θ_h of 5 m relative to the embankment geometry, as shown in Fig. 6a, the deterministic result can give a relatively conservative estimation of the possible quantity of flow rate. The computed random results are distributed within a small range being represented by a low coefficient of variation. This is probably because that when the water flow passes through the soils with random permeability, it is more likely to flow along the zones of higher permeability. On the basis of this fact, since a relatively small correlation length is considered, it may lead to a limited variation of the permeability field for each realization as a whole. It can be seen from Fig. 6b that the increase of the correlation length leads to an increase in the coefficient of variation of these random results. Although the position of soils with low or high permeability is different in each simulation, the water is generally more concentrated due to the better continuity of soils of higher permeability, which can affect the quantity of the total flow rate through the embankment. This effect becomes more apparent when the correlation length is 20 m as illustrated in Fig. 6c, and it leads to a greater coefficient of variation of flow rate than that of the above two cases. Under such a scenario, the difference in the resulted flow rate depends largely on each realization of the permeability field; therefore, the larger the areas of higher permeability in one realization, the greater the computed flow rate.

For all the cases applied with a water level of 9 m but under various correlation lengths, the histogram distributions of the resulted normalized flow rate shown in Figs. 6d–f are highly similar to that from the corresponding cases with a 7 m water level (see Figs. 6a–c). Such a high similarity in terms of these dimensionless results may be attributed to a fact that the same sample of the permeability field is utilized in a sequence of realizations of Monte Carlo simulations. By use of the consistency of the basic tend presented in Fig. 6, the dimensionless results of flow rate can be used reasonably for probabilistically evaluating the seepage performance of embankments with other water levels that are not considered in this study, with a combination of the corresponding deterministic coupled result.

4.3   Seepage Pattern

Figure 7 shows the profiles of seepage patterns occurred in random soils with different correlation lengths for the embankments applied with a water level of 7 m, which are illustrated based on a typical realization of random field for each scenario presented. For a better understanding, three vertical cross-sections (i.e. sections of *A-A*, *B-B* and *C-C*
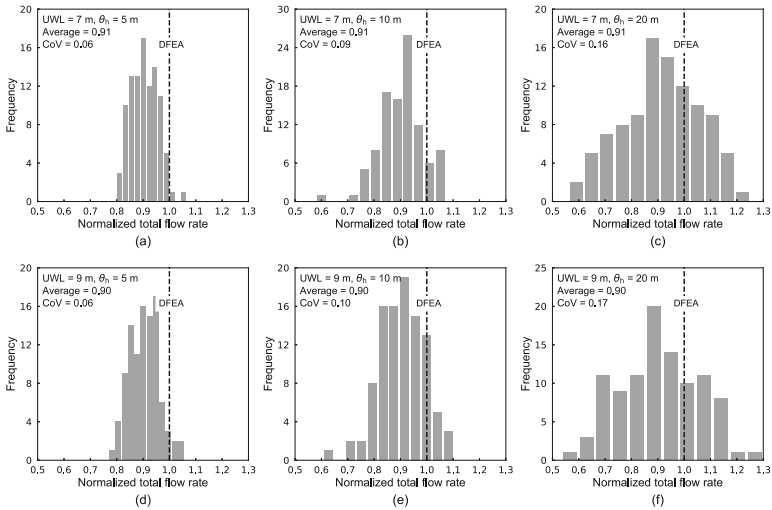
Fig. 6. Histograms of normalized total flow rate for embankments with different combinations of upstream water level (UWL) and horizontal correlation length (θ_h). CoV = coefficient of variation; DFEA = deterministic finite element analysis. The value of coefficient of permeability used in the DFEA is the arithmetic average of the uniform distribution, as listed in Table 1b.

as depicted in Fig. 7a) across the embankment model at different locations are selected to provide more details of the internal variation of water flow.

For a small value θ_h of 5 m as shown in Fig. 7a, the flow path of the water is significantly affected by the non-uniform soils with random permeability. As expected, the water flows more easily along those regions of higher permeability, which leads to a grossly irregular seepage pattern differing from the deterministic case shown in Fig. 5a. For the soils with lower permeability near the upstream surface, it has certain positive effects on preventing the water from entering into the embankment. This effect may be more apparent and controlled when it uses a 2D model that is essentially a cross-section of a 3D embankment. According to the overall velocity vectors distribution at the exit, the permeability field also greatly affects the maximum exit gradient reflecting the local seepage behavior, but of which the estimation of the maximum exit gradient is beyond the scope of this study. When a slightly larger correlation length θ_h of 10 m is considered, as shown in Fig. 7b, a more horizontally continuous flow pattern can be observed throughout each vertical cross-section of the embankment. Such a situation provides a more direct channel for the water flow, although the areas of lower permeability are also relatively larger. Another scenario is also possible that the regions of low permeability is greater than that of high permeability, which can reduce the quantity of total flow rate passing through the embankment. For the case considering a θ_h of 20 m shown in Fig. 7c, the locations of concentrated water flow change more significantly due to the greater blocked effect of soil regions with lower permeability. The variation of flow rate depends largely on the realization of permeability field in which it is likely to obtain a smaller or larger flow rate, which can be inferred from the results shown in Fig. 6c.

For the cases with a 9 m water level, the corresponding seepage patterns at each cross-section of the embankment are presented in Fig. 8, where its realizations of permeability field under various correlation lengths remain the same as shown in Fig. 7. Comparison of these contours between Figs. 7 and 8 shows that the rise of water level mainly affects the flow pattern on the upper part of the embankment and increases the magnitude of velocity vectors at the exit positions, which is consistent with most of the observations and measured data from an engineering site. Under such a situation of raising water level, the resulted flow rate will also increase obviously as presented in Figs. 5 and 6. These results of seepage patterns in various scenarios explained above can serve as a valuable basis for reducing the risk of seepage failure of a soil embankment subjected to fluctuation in water level.
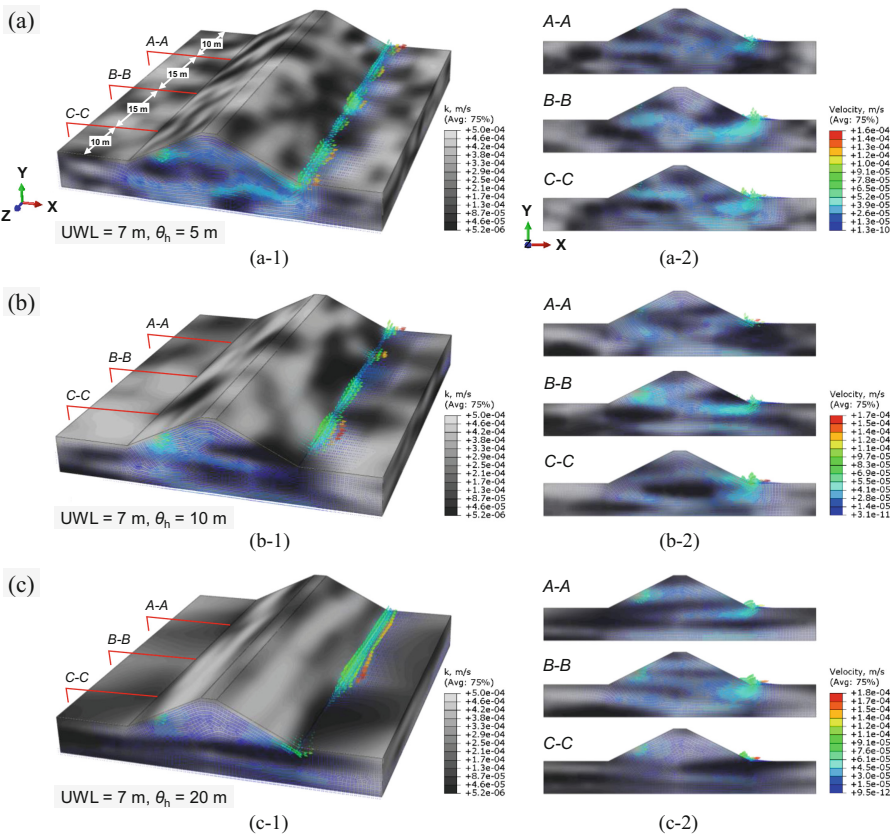

Fig. 7. Velocity vectors of seepage in random soils with a horizontal correlation length of (a) 5 m, (b) 10 m, and (c) 20 m for the embankment applied with a 7 m water level. UWL = upstream water level; θ_h = horizontal correlation length.
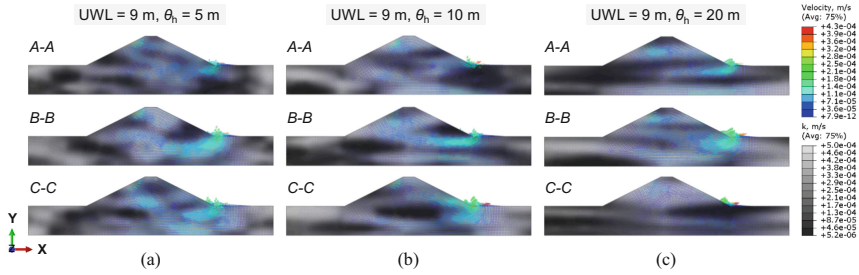
Fig. 8. Velocity vectors of seepage in random soils with a horizontal correlation length of (a) 5 m, (b) 10 m, and (c) 20 m at each cross-section of the same realization shown in Fig. 7 for the embankment applied with a 9 m water level.

4.4 Failure Mechanism

Figure 9 shows the contours of maximum principal plastic strain for the embankments subjected to different water levels, of which the case with a 5 m water level presented in Fig. 9a is considered as a comparison example. Note that the failure modes of all the random models under various water levels are basically identical with the corresponding deterministic cases. The main reason for this phenomenon may be attributed to the failure mechanism that, the rise of a certain water level results in the increase of pore water pressure applied on the soil skeletons near the toe of the upstream slope, and the shear strength of the soils is then reduced in accordance with the principle of effective stress. This statement can be exemplified indirectly by the result of the case with the same water level at the upstream and downstream sides of the embankment (see Fig. 9a), in which two basically symmetrical failure modes can be observed and the overall stability of this embankment represented by a factor of safety of 1.62 is much better than the other scenarios. In accordance with the non-convergence of finite element program, with the increase of water level, the shear strength of the soils in those regions of higher pore water pressure will be faster to reach a threshold value in the process of strength reduction operation. For this reason, the shear failure zones of an embankment with higher water level will be reduced in different degree and a corresponding smaller factor of safety can be obtained associated with the failure state (see Figs. 9b and c).

Another issue related to the coupled performance is the effect of internal uneven seepage forces caused by the random soil permeability on the stability of the embankment. Based on the results of irregular seepage patterns described earlier, a greater seepage force may be likely generated in the soil regions of higher permeability due to the faster speed of water flow, which may result in some local seepage failures in reality, such as piping. Although this fact is relatively important from a practical viewpoint, in the numerical coupled analysis the overall stability of an embankment depends mainly on the shear strength of soils. Therefore, a rise of water level plays a more dominant role in inducing the stability failure of an embankment than the irregular seepage force acted on the soils.
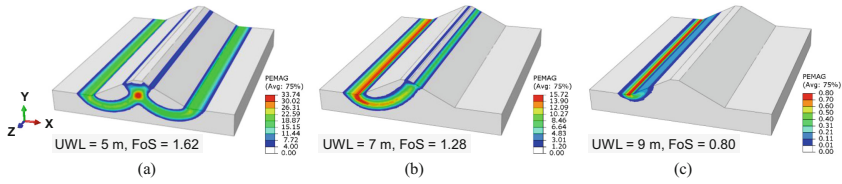
Fig. 9. Failure modes and the corresponding factors of safety for the embankments under various water levels of (a) 5 m, (b) 7 m, and (c) 9 m. UWL = upstream water level; FoS = factor of safety.

5   Concluding Remarks

The coupled solutions of a large-scale 3D soil embankment subjected to water level fluctuation are evaluated by using the random finite element method in this study. The soil permeability controlling the seepage behavior is considered as spatially variable, being represented by a random field with a uniform distribution. The histogram results of normalized total flow rate indicate that the horizontal correlation length of the permeability field has significant effects on the seepage response; that is, the variability of the obtained flow rate increases with the increase of correlation length. This is mainly due to the effect of irregular seepage patterns caused by the heterogeneous soil permeability. The profiles of seepage velocity vectors in random soils demonstrate that the water is more likely to flow along the regions of higher permeability and a relatively concentrated flow field then is formed, especially when a greater correlation length is considered in the analysis. The contour results also show that in the same site the variation of water level mainly affects the seepage pattern near the upstream part of an embankment. In addition, the failure mechanism indicates that a rise of water level plays a dominant role in leading to the instability of the embankment compared with the generated irregular seepage force, due mainly to the great reduction of the effective stress of soil skeletons near the upstream slope toe. The factor of safety of the embankment decreases with the increase of upstream water level, and the corresponding failure mode changes significantly. The investigated results from this study contribute to the design or reinforcement of a soil embankment and serve as a basis of the green cycle and sustainable development of embankment engineering.

This study mainly highlights the effect of spatial heterogeneity in soil permeability, whereas the shear strength parameters of soils are treated as constant. However, the soil strength should also be spatially varying in different degree, which may affect the global stability of an embankment (e.g. Ji and Chan 2014; Liu et al. 2018). Moreover, transient-state analysis considering the dynamic hydraulic head is desirable as it may replicate the factual failure mechanism in high flow speed conditions. These issues form strands of future works.

References

Chen, J.: Breaching of Lianfeng reservoir in Xinjiang due to leakage. Chinanews (2013). http://www.chinanews.com/tp/hd2011/2013/02-02/171499.shtml

Chen, W.T.: Crevasse rescue of embankment in the east and west sides of Poyang Lake. Bjnews (2020). https://www.bjnews.com.cn/detail/159464002415876.html

Cho, S.E.: Probabilistic analysis of seepage that considers the spatial variability of permeability for an embankment on soil foundation. Eng. Geol. **133–134**, 30–39 (2012)

Fenton, G.A., Griffiths, D.V.: Risk Assessment in Geotechnical Engineering. Wiley, Hoboken (2008)

Grigoriu, M.: Applied Non-Gaussian Processes: Examples, Theory, Simulation, Linear Random Vibration, and MATLAB Solutions. Prentice-Hall International (UK) Limited, London (1995)

Griffiths, D.V., Fenton, G.A.: Three-dimensional seepage through spatially random soil. J. Geotech. Geoenviron. Eng. **123**(2), 153–160 (1997)

Gholami Korzani, M., Galindo-Torres, S.A., Scheuermann, A., Williams, D.J.: Smoothed Particle hydrodynamics for investigating hydraulic and mechanical behaviour of an embankment under action of flooding and overburden loads. Comput. Geotech. **94**, 31–45 (2018)

Ji, J., Chan, C.L.: Long embankment failure accounting for longitudinal spatial variation – a probabilistic study. Comput. Geotech. **61**, 50–56 (2014)

Jia, G.W., Zhan, T.L.T., Chen, Y.M., Fredlund, D.G.: Performance of a large-scale slope model subjected to rising and lowering water levels. Eng. Geol. **106**(1–2), 92–103 (2009)

Liu, Y., Lee, F.H., Quek, S.T., Beer, M.: Modified linear estimation method for generating multi-dimensional multi-variate Gaussian field in modelling material properties. Probab. Eng. Mech. **38**, 42–53 (2014)

Liu, Y., Zhang, W., Zhang, L., Zhu, Z., Hu, J., Wei, H.: Probabilistic stability analyses of undrained slopes by 3D random fields and finite element methods. Geosci. Front. **9**(6), 1657–1664 (2018)

Li, Z., Ye, W., Marence, M., Bricker, J.: Unsteady seepage behavior of an earthfill dam during drought-flood cycles. Geosciences **9**(1), 17 (2018)

Phoon, K.K., Kulhawy, F.H.: Evaluation of geotechnical property variability. Can. Geotech. J. **36**(4), 625–639 (1999)

Qi, S., Vanapalli, S.K.: Hydro-mechanical coupling effect on surficial layer stability of unsaturated expansive soil slopes. Comput. Geotech. **70**, 68–82 (2015)

Rivera-Hernandez, X.A., Ellithy, G.S., Vahedifard, F.: Integrating field monitoring and numerical modeling to evaluate performance of a Levee under climatic and tidal variations. J. Geotech. Geoenviron. Eng. **145**(10), 05019009 (2019)

Swiss Standard SN 670 010b: Characteristic coefficients of soils. Association of Swiss Road and Traffic Engineers, Zurich (1999)

Srivastava, A., Babu, G.L.S., Haldar, S.: Influence of spatial variability of permeability property on steady state seepage flow and slope stability analysis. Eng. Geol. **110**(3–4), 93–101 (2010)

Wang, M.Y., Liu, Y., Ding, Y.N., Yi, B.L.: Probabilistic stability analyses of multi-stage soil slopes by bivariate random fields and finite element methods. Comput. Geotech. **122**, 103529 (2020)

Yu, X.: Bursting of embankment in Leizhou Younth Canar in Guangdong Province. Chinadaily (2014). http://cnews.chinadaily.com.cn/2014-05/21/content_17528086.htm

Zhang, L., Wu, F., Zheng, Y., Chen, L., Zhang, J., Li, X.: Probabilistic calibration of a coupled hydro-mechanical slope stability model with integration of multiple observations. Georisk Assess. Manage. Risk Eng. Syst. Geohazards **12**(3), 169–182 (2018)